JOURNAL OF CATALYSIS 146, 335–345 (1994)

Effect of Additives on the Structure and Reactivity of the Surface Vanadium Oxide Phase in V_2O_5/TiO_2 Catalysts

Goutam Deo and Israel E. Wachs[1]

Zettlemoyer Center for Surface Studies, Department of Chemical Engineering, Lehigh University, Bethlehem, Pennsylvania 18015, USA

Received February 26, 1993; revised November 1, 1993

Additives on a 1% V_2O_5/TiO_2 catalyst exhibit two types of interactions with the surface vanadium oxide phase which are observed by Raman spectroscopy under dehydrated conditions and methanol oxidation. Under dehydration conditions, noninteracting additives (WO_3, Nb_2O_5, and SiO_2) coordinate directly to the oxide support without significantly interacting with the surface vanadium oxide phase. Furthermore, the effect of the noninteracting additives on the surface vanadium oxide phase is independent of the order of preparation or precursor used. These noninteracting additives do not affect the methanol oxidation activity and selectivity. Interacting additives (K_2O and P_2O_5), however, directly coordinate with the surface vanadium oxide phase. Addition of K_2O progressively titrates the surface vanadium oxide sites, as observed from the changes in the structure and reactivity of the surface vanadium oxide phase. The effect of P_2O_5 on the surface vanadium oxide phase depends on the concentration and sequence of preparation. Addition of higher concentrations of P_2O_5 forms vanadium phosphate compounds, and results in a change in methanol oxidation activity and selectivity. The addition of 1% V_2O_5 to a 5% P_2O_5/TiO_2 sample, however, does not show any evidence of compound formation, but a part of the surface vanadium oxide phase appears to be titrated. Under ambient conditions, the additives change the pH at point of zero charge of the surface moisture layer which controls the structure of the surface vanadium oxide layer. Thus, depending on the nature of the additive, interacting or noninteracting, the dehydrated structure and reactivity toward methanol oxidation of the surface vanadium oxide phase are affected or remain essentially unchanged, respectively.

INTRODUCTION

Supported vanadia–titania catalysts typically used in industry and research usually contain various additives (impurities and promoters) that are intentionally or unintentionally added (1–3). The oxides of tungsten, niobium, silicon, potassium, and phosphorous are some of the main additives usually considered for supported vanadium oxide catalysts. Tungsten oxide and niobium oxide are used as promoters for the selective catalytic reduction of NO_x. Silica is typically present as an impurity on titania. Potassium and phosphorous oxides are considered poisons for certain reactions, but also increase the selectivity for certain hydrocarbon oxidation reactions. In essence some of these additives are detrimental to the catalytic oxidation properties, whereas others are necessary to obtain maximum catalytic efficiency. Furthermore, only a critical amount of additive is usually necessary to form the active catalyst. A brief literature review of the influence of additives upon V_2O_5/TiO_2 catalysts is presented below.

Van Hengstum *et al.* (4) observed that the influence of phosphorous and potassium additives on V_2O_5/TiO_2 catalysts depended on the type of hydrocarbon oxidized. For the selective oxidation of toluene, the additives had a large negative effect on the activity and yield of benzoic acid. For the oxidation of *o*-xylene, the additives had a negative effect for low vanadium oxide contents, but the presence of additives improved the catalyst efficiency at high vanadium oxide contents. The addition of phosphorous increased the surface acidity of the V_2O_5/TiO_2 catalysts since the acid side reactions were enhanced. Potassium altered the nature of the active sites, which was attributed to the possible formation of amorphous bronzes between vanadium oxide and potassium. The presence of amorphous bronzes was concluded since bulk V_2O_5 features were not observed in the Raman spectra at loadings in slight excess of monolayer amounts. The presence of potassium on the V_2O_5/TiO_2 catalysts also increased the T_{max} temperature in temperature programmed reduction experiments, and the presence of phosphorous only slightly influenced the T_{max} temperature. This study, however, did not provide structural information about the surface vanadium oxide phase in the presence of the potassium and phosphorous additives.

Zhu and Andersson (5, 6) studied the effect of potassium and phosphorous additives on a 2 wt.% V_2O_5/TiO_2 catalyst for the oxidation of toluene, and observed that the oxidation activity decreased rapidly as the additives were deposited. The addition of potassium decreased the selectivity of the oxidative coupling and acid side reaction, and increased the formation of carbon oxides. The addi-

[1] To whom correspondence should be addressed.

0021-9517/94 $6.00

tion of phosphorous increased the selectivity of oxidative coupling products and carbon oxides, and decreased the selectivity to side-chain oxidation products. Characterization of the surface vanadium oxide phase in the potassium- and phosphorous-doped V_2O_5/TiO_2 catalyst by X-ray photoelectron and infrared spectroscopy, and X-ray diffraction indicated that the additives (phosphorous and potassium) and vanadium oxide are highly dispersed at low additives concentrations. The formation of small quantities of KVO_3 for K/V ratios of ≥ 1 were detected from the X-ray powder diffraction pattern. Potassium in excess of the amount bonded to vanadium resulted in a decrease in surface area and an increase in the anatase-to-rutile transformation. Addition of phosphorous, in excess of the P/V ratio of 1.25, resulted in agglomeration of the phosphorous–vanadium–oxygen phase and the formation of vanadium phosphate compounds which were detected by XRD. In contrast to the potassium additives, the phosphorous-doped V_2O_5/TiO_2 catalyst remained unchanged and so did the anatase-to-rutile ratio.

Bond and Tahir (7) investigated the influence of potassium and phosphorous on V_2O_5/TiO_2 catalysts for the oxidation of butadiene. The addition of phosphorous had little effect on the catalyst reducibility or activity for butadiene oxidation. The addition of potassium decreased the catalyst reducibility and activity for butadiene oxidation. Structural information of the surface vanadium oxide phase upon deposition of the additives was not obtained.

Vuurman *et al.* (8) characterized the V_2O_5–WO_3/TiO_2 system in detail using Raman spectroscopy obtained under ambient and dehydrated conditions. Under ambient conditions, the structure of the surface vanadium oxide species in the presence of tungsten oxide depended on the surface pH at point of zero charge (pzc). Under dehydrated conditions, the surface vanadium oxide and tungsten oxides on TiO_2 were present as separate species, and, essentially, were not influenced by the second surface metal oxide at all loadings. The sequence of impregnation of the vanadium oxide and tungsten oxide did not change the nature of the surface vanadium oxide and surface tungsten oxide species.

Ramis *et al.* (9) also examined the V_2O_5–WO_3/TiO_2 system by infrared spectroscopy under dehydrated conditions and observed the presence of V=O and W=O vibrations exactly in the same position as the individual supported metal oxide systems (V_2O_5/TiO_2 and WO_3/TiO_2). From these results they concluded that the surface vanadium oxide and tungsten oxide do not strongly interact with each other.

Chen and Yang have studied the effect of WO_3 on the V_2O_5/TiO_2 catalysts for the selective catalytic reduction (SCR) of nitric oxide with ammonia (10). They observed that the addition of WO_3 increases the activity of the SCR reaction and significantly increases the poison resistance of the WO_3–V_2O_5/TiO_2 catalysts to alkali and arsenious oxides. An increase in the Brønsted acidity was observed upon the addition of WO_3 to the V_2O_5/TiO_2 catalyst. The Brønsted acid sites were proposed to be the active sites for the SCR reaction. No structural characterization of the surface vanadium oxide phase was performed and all the conclusions were based on catalytic reaction data.

The studies above suggest that the various additives can influence the behavior of the V_2O_5/TiO_2 catalysts differently. However, none of the studies has attempted to correlate the structure of the surface vanadium oxide phase with the catalytic activity of the supported vanadium oxide catalysts in the presence of the various additives. Such a structure–reactivity relationship is critical to the fundamental understanding of the influence of the additives on the V_2O_5/TiO_2 catalytic system. For this reason, the purpose of this study is to add different additives (WO_3, Nb_2O_5, SiO_2, P_2O_5, and K_2O) to a 1% V_2O_5/TiO_2 catalyst and to observe the changes in the structure and reactivity of the surface vanadium oxide phase by Raman spectroscopy and methanol oxidation, respectively. Models of the interactions of the various additives with the surface vanadium oxide phase are developed by correlating the structure and reactivity of the surface vanadium oxide phase in the presence and absence of the additives.

EXPERIMENTAL

Catalyst Preparation

The support material used for this study was TiO_2 (Degussa, P-25) with a surface area of 50 m^2/g and an anatase-to-rutile ratio of 95 : 5. The support was calcined at 450°C for 16 hr and sieved to <75 μm prior to the preparation of the catalysts.

Supported vanadium oxide on TiO_2 was prepared by the incipient wetness impregnation of vanadium triisopropoxide oxide (Alfa, 95–98% pure) precursor in a methanol solution. An equivalent amount of vanadium triisopropoxide oxide to form 1% V_2O_5 by weight was added to known amounts of methanol to form a solution for the incipient wetness impregnation method. The impregnated catalysts were thoroughly mixed and dried at room temperature for 16 hr in a glove box under a nitrogen environment. Room temperature drying for 16 hr was followed by drying at 100–120°C under flowing nitrogen for 16 hr. Finally the catalysts were dried at 450°C for 2 hr in flowing oxygen (or air). The final catalysts were denoted as 1% V_2O_5/TiO_2.

Tungsten oxide, niobia, silica, potassium oxide, and phosphorous oxide were added in order to study the

TABLE 1

Precursors and Solvents Used for Impregnation of the Additives

Additives on 1% V_2O_5/TiO_2	Precursor	Solvent
Tungsten oxide	Ammonium metatungstate	Water
Niobia	Niobium ethoxide and	Propanol
	Niobium oxalate	Water
Silica	Tetramethyl orthosilicate	Methanol
Potassium	KOH solution (1–3 wt.%)	Water
Phosphorous	Dilute H_3PO_4 (3–4 wt.%)	Water

effect of additives on the 1% V_2O_5/TiO_2 sample. The amounts of the additives were limited to monolayer loadings in most cases since at these loadings the surface vanadium oxide phase would be most influenced. The precursors and solvents used to deposit the respective additives on the 1% V_2O_5/TiO_2 catalyst are listed in Table 1.

Niobia and silica were deposited on the 1% V_2O_5/TiO_2 sample by nonaqueous impregnation of a solution of the respective precursors and solvents shown in Table 1. The drying and heating of the samples were performed under conditions similar to those for the 1% V_2O_5/TiO_2 sample. Tungsten oxide, potassium oxide, and phosphorous oxide were deposited on the 1% V_2O_5/TiO_2 sample by aqueous impregnation of a solution of the respective precursors and water (see Table 1). Niobia was also deposited on the 1% V_2O_5/TiO_2 by the aqueous impregnation method using double impregnation of 3% Nb_2O_5 each time. Calcination of these catalysts was done under similar temperatures as before, except that the atmosphere was always oxygen (or air) instead of nitrogen in the drying stage. These catalysts were denoted as $z\%\ M_xO_y/1\%\ V_2O_5/TiO_2$, where $z\%\ M_xO_y$ stands for the weight percent of the additive deposited on the previously prepared 1% V_2O_5/TiO_2 sample.

Some catalysts were also prepared in the reverse sequence. For example, known amounts of niobium ethoxide and propanol, corresponding to 3% Nb_2O_5 and incipient impregnation volume, were first deposited on the TiO_2 support, then dried in nitrogen at room temperature and 120°C, and calcined at 450°C in air or oxygen. Known amounts of vanadium triisopropoxide oxide and methanol solution corresponding to 1% V_2O_5 were added to the 3% Nb_2O_5/TiO_2 sample by incipient wetness impregnation, followed by the necessary drying and calcination. Such samples were denoted as $1\%\ V_2O_5/z\%\ M_xO_y/TiO_2$, where $z\%\ M_xO_y$ stands for the weight percent of the additive deposited initially on the TiO_2 support.

Raman Spectrometer

The laser Raman spectra were obtained with an Ar^+ laser (Spectra Physics, Model 2020-50). The incident laser line delivered 1–20 mW of power measured at the sample and tuned to 514.5 nm. The scattered radiation from the sample was directed into an OMA III (Princeton Applied Research, Model 1463) optical multichannel analyzer with a photodiode array detector thermoelectrically cooled to −35°C. About 100–200 mg of the pure catalysts were made into wafers and placed in the *in situ* cell. The *in situ* cell consisted of a stationary sample holder, which has been described elsewhere (8). The *in situ* cell was heated to 300°C for ½ hr and then cooled to room temperature before the Raman spectra were obtained. The entire procedure was performed in a stream of flowing oxygen (ultra high purity grade) over the catalyst sample to ensure complete oxidation of the catalysts. The Raman spectra of the catalysts were also obtained under ambient conditions to check for the effect of hydration–dehydration treatments and compound/crystallite formation.

Methanol Oxidation Reaction

A reactant gas mixture of $CH_3OH/O_2/He$ in the molar ratio of ~6/13/81 was used for the methanol oxidation reaction. The oxygen/helium mixture from two mass flow controllers (Brooks) was bubbled through a saturator containing methanol operating at ~9.5°C by flowing cooled water obtained from a Neslab cooler (RTE 110A). The total gas flow rate was maintained at ~100 standard cubic centimeter per minute (sccm) for all the catalytic runs. The gas flow through the differential reactor was from top to bottom. The reactor was held vertical and made out of Pyrex glass of 6.2 mm outer diameter. The temperature around the reactor was maintained by a furnace (Linberg) connected to a temperature controller (Eurotherm). The outlet of the reactor to the gas chromatograph (HP 5840A) was heated to 120–130°C. Analysis of the reactants and the products was performed on the GC using two TCDs and a FID with two packed columns (Poropak R and Carbosieve SII) connected in parallel. The amount of catalyst was controlled to achieve less than 10% methanol conversion in order to maintain differential reaction conditions and eliminate problems due to heat and mass transfer. The product data were collected for 4–5 hr and checked for any rapid deactivation. The total conversion of methanol was found not to vary by more than 10% over the 4–5 hr. The conversion data obtained after 10–20 min were used to calculate the turnover frequency (TOF) as they are most representative of the structural data obtained in a fully oxidized atmosphere. Three to five sets of data were obtained for all the catalysts, and the average value of the activity and selectivity is presented. The

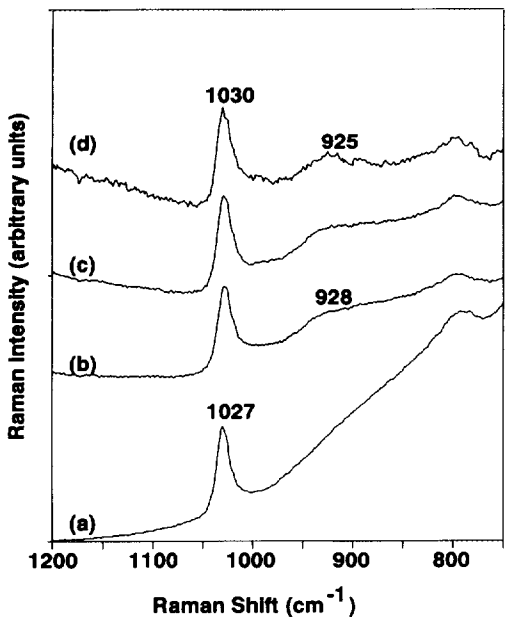

FIG. 1. Raman spectra of niobium oxide-doped 1% V_2O_5/TiO_2 system. Spectra obtained under dehydrated conditions. (a) 1% V_2O_5/TiO_2; (b) 3% Nb_2O_5/1% V_2O_5/TiO_2 (aq.); (c) 6% Nb_2O_5/1% V_2O_5/TiO_2 (aq.); (d) 6% Nb_2O_5/1% V_2O_5/TiO_2 (non-aq.).

turnover frequency (units $\equiv s^{-1}$) was calculated from the total moles of methanol converted per mole of vanadium atom present per second.

RESULTS

Raman Spectra

Niobia–vanadia–titania system. The Raman spectra of the series of niobia-promoted 1% V_2O_5/TiO_2 catalysts are shown in Fig. 1 in the 700–1200 cm^{-1} region. The intense vibrations of the TiO_2 support dominate the spectrum below 700 cm^{-1} and are not shown. The spectrum of the 1% V_2O_5/TiO_2 catalyst is included for reference. The Raman spectrum of unpromoted 1% V_2O_5/TiO_2 exhibits a band at 1027 cm^{-1} and a peak at 790 cm^{-1}. The latter peak arises from titanium–oxygen vibrations and exists in the Raman spectrum of the pure TiO_2 support (8). None of the Raman spectra of the niobia-doped 1% V_2O_5/TiO_2 catalysts shows the Raman features arising from niobium–oxygen vibrations. This is due to the low cross section of the niobium–oxygen vibrations compared to the vanadium-oxygen vibrations. The Raman spectra of 6% Nb_2O_5/TiO_2 under dehydrated conditions exhibit Raman bands at 985 and 930 cm^{-1} (11). The Raman band at 1027 cm^{-1} is due to the vanadium-oxygen terminal vibration of the surface vanadium oxide species on TiO_2 (8, 12). As 3 and 6% Nb_2O_5 are added to the previously prepared 1% V_2O_5/TiO_2 catalyst by aqueous impregnation (niobium oxalate and water; final calcination at 450°C in oxygen), the Raman band at 1027 cm^{-1} shifts to 1030 cm^{-1}, and a broad Raman feature is observed at 920–930 cm^{-1} arising from additional vanadium oxygen vibrations. The assignment of the 920–930 cm^{-1} Raman band to the vanadium–oxygen vibration rather than the niobium–oxygen vibration is due to the absence of any niobium–oxygen vibration at 985 cm^{-1}. Addition of 6% Nb_2O_5 to previously prepared 1% V_2O_5/TiO_2 by nonaqueous impregnation (niobium ethoxide and propanol; final calcination at 450°C in oxygen) shows the presence of Raman bands at 1030 and ~930 cm^{-1}, which is similar to the Raman features observed for the aqueous impregnation of niobium oxide. The Raman spectrum of 1% V_2O_5 added to previously prepared 3% Nb_2O_5/TiO_2 shows the presence of the Raman features due to the vanadium oxygen vibrations at 1030 and 925 cm^{-1}. The Raman spectra of the various dehydrated niobia-doped 1% V_2O_5/TiO_2 samples are different from the corresponding Raman spectra obtained under ambient conditions. Under ambient conditions, the Raman bands due to the surface vanadium oxide phase on titania are shifted from ~950 cm^{-1} to ~980 cm^{-1} when niobia is added. No Raman features of bulk V_2O_5 and Nb_2O_5 are present in any of the spectra. Monolayer loadings of the Nb_2O_5/TiO_2 and V_2O_5/TiO_2 systems correspond to ~7% Nb_2O_5 and 6% V_2O_5, respectively (8, 11, 12).

Tungsten oxide–vanadia–titania system. The Raman spectrum of 7% $WO_3/V_2O_5/TiO_2$ catalysts is shown in Fig. 2 in the 700–1200 cm^{-1} region along with the spectrum of 1% V_2O_5/TiO_2 for reference. The Raman spectrum of 7% WO_3/1% V_2O_5/TiO_2 shows the presence of two sharp features at 1030 and 1010 cm^{-1}, and a broad Raman band at 925 cm^{-1}. The Raman spectra of 7% WO_3/TiO_2 show Raman features at 1010 cm^{-1} due to the W=O vibration (8). Hence, the Raman band at 1010 cm^{-1} for the 7% WO_3/1% V_2O_5/TiO_2 sample is due to the W=O vibration, and the remaining bands at 1030 and 930 cm^{-1} are due to the vanadium-oxygen vibrations. Similar to the niobia–vanadia–titania system, the Raman band of the vanadium oxygen terminal vibration of the surface vanadium oxide phase is shifted from 1027 to 1030 cm^{-1} and a broad band appears at 930 cm^{-1}. A previous detailed investigation by Vuurman *et al.* of the tungsten–vanadia–titania system shows that the sequence of impregnation of the vanadium oxide and tungsten oxide does not change the Raman spectra of the surface vanadium oxide and tungsten oxide phases (8). No features of bulk V_2O_5 or bulk WO_3 are observed for the 7% WO_3/1% V_2O_5/TiO_2 sample. Monolayer loadings of the WO_3/TiO_2 system correspond to ~8% WO_3 (8). The Raman spectra obtained under dehy-

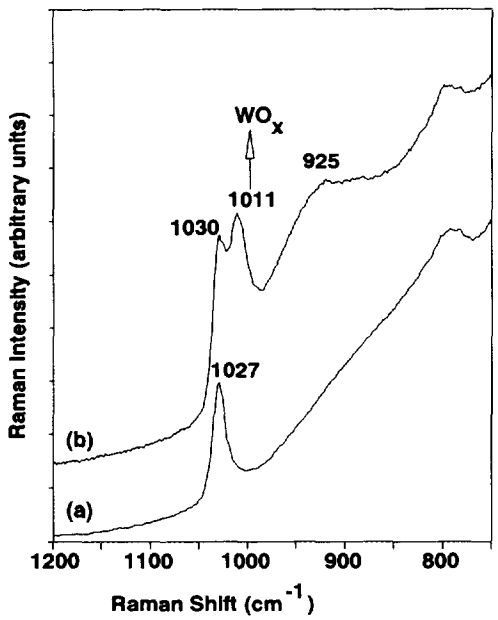

FIG. 2. Raman spectra of tungsten oxide-doped 1% V_2O_5/TiO_2 system. Spectra obtained under dehydrated conditions. (a) 1% V_2O_5/TiO_2; (b) 7% WO_3/1% V_2O_5/TiO_2.

drated conditions of these samples (Fig. 2) are different from the corresponding Raman spectra obtained under ambient conditions, and the Raman band of the surface vanadium oxide phase shift from ~950 to ~980 cm^{-1} when tungsten oxide is added.

Silica–vanadia–titania. The Raman spectrum after the addition of 3% SiO_2 to a previously prepared 1% V_2O_5/TiO_2 catalyst is presented in Fig. 3 and the Raman spectrum of 1% V_2O_5/TiO_2 is shown for reference. Monolayer loadings of SiO_2 on TiO_2 have not been determined, but 3% SiO_2 corresponds to ~0.8 monolayers of V_2O_5 on TiO_2 on an equimolar basis. The Raman spectrum of 3% SiO_2/1% V_2O_5/TiO_2 shows a slight downward shift of the band from 1027 to 1024 cm^{-1} due to the addition of silica. No evidence of the broad Raman feature at 925–930 cm^{-1} or features of bulk V_2O_5 are observed. Dehydration experiments of the 3% SiO_2/TiO_2 sample are not very conclusive since a change in the Raman spectra during hydration and dehydration conditions is not evident (13). The presence of bulk SiO_2 cannot be excluded since bulk SiO_2 possesses weak and broad bands in the 700–1200 cm^{-1} region and, hence, may not be observable. The Raman band under ambient conditions of the vanadium oxide phase in the 3% SiO_2/1% V_2O_5/TiO_2 sample is similar to the Raman band of the 1% V_2O_5/TiO_2 sample (~940 cm^{-1}). Decreasing the amount of SiO_2 (1% SiO_2) in the 1% V_2O_5/TiO_2 sample does not provide any additional information since essentially the same Raman spectra are observed under ambient and dehydrated conditions.

Potassium oxide–vanadia–titania. The Raman spectra of various amounts of K_2O added to 1% V_2O_5/TiO_2 are shown in Fig. 4 in the 700–1200 cm^{-1} region along with 1% V_2O_5/TiO_2 as reference. Various loadings of K_2O were investigated because of the pronounced influence of K_2O on the Raman spectra of 1% V_2O_5/TiO_2. Addition of 0.05% K_2O shifts the Raman band of the terminal V=O bond from 1027 to 1025 cm^{-1}, and a new broad shoulder appears at 1001 cm^{-1}. Larger amounts of K_2O further shift the Raman band of the V=O bond to lower wavenumbers (from 1027 to 1009 cm^{-1}) and increase the relative intensity of the broad Raman features in the 980–1000 cm^{-1} region. The Raman bands obtained under ambient conditions of the potassium-doped 1% V_2O_5/TiO_2 samples occur at lower wavenumbers (880–910 cm^{-1}) compared to the undoped 1% V_2O_5/TiO_2 sample (~950 cm^{-1}), and are different from the corresponding Raman spectra obtained under dehydrated conditions.

Phosphorous oxide–vanadia–titania. Various combinations and sequences of the preparation of P_2O_5 and 1% V_2O_5 deposited on TiO_2 are shown in Fig. 5 along with the spectrum of 1% V_2O_5/TiO_2 as reference. Addition of 1% P_2O_5 to previously prepared 1% V_2O_5/TiO_2 shows a slight shift along with broadening of the Raman band at

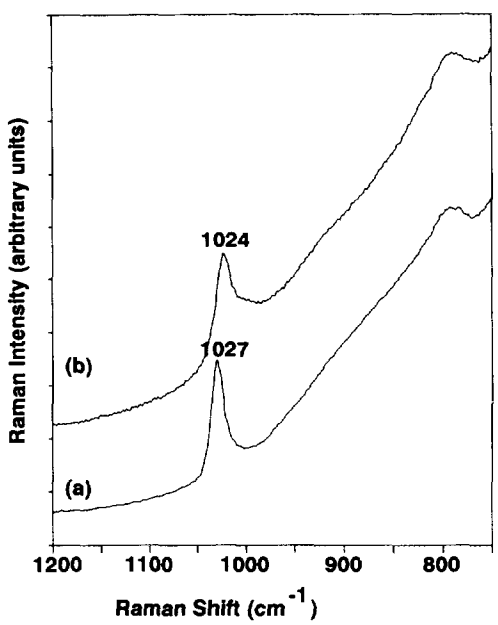

FIG. 3. Raman spectra of silica-doped 1% V_2O_5/TiO_2 system. Spectra obtained under dehydrated conditions. (a) 1% V_2O_5/TiO_2; (b) 3% SiO_2/1% V_2O_5/TiO_2.

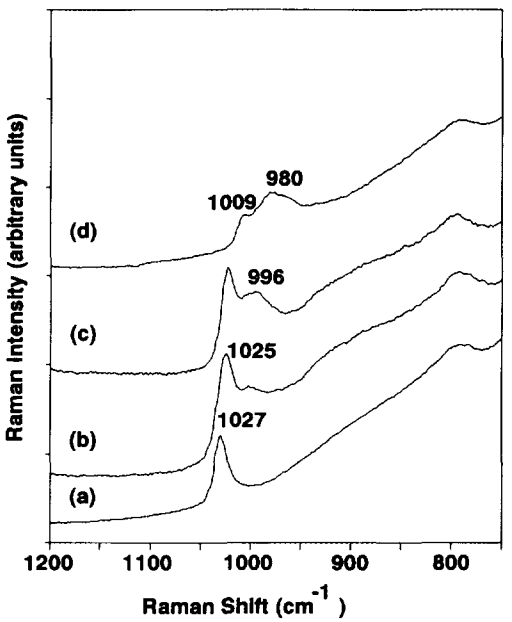

FIG. 4. Raman spectra of potassium-doped 1% V_2O_5/TiO_2 system. Spectra obtained under dehydrated conditions. (a) 1% V_2O_5/TiO_2; (b) 0.05% K_2O/1% V_2O_5/TiO_2; (c) 0.2% K_2O/1% V_2O_5/TiO_2; (d) 0.7% K_2O/1% V_2O_5/TiO_2.

1027 cm^{-1} due to the V=O bond. Addition of 3% P_2O_5 to previously prepared 1% V_2O_5/TiO_2 shows two relatively intense and broad Raman bands at 1035 and 923 cm^{-1}. The Raman bands of 3% P_2O_5 on 1% V_2O_5/TiO_2 are the same when obtained under ambient conditions, and closely correspond to the Raman bands of bulk α_1-$VOPO_4$

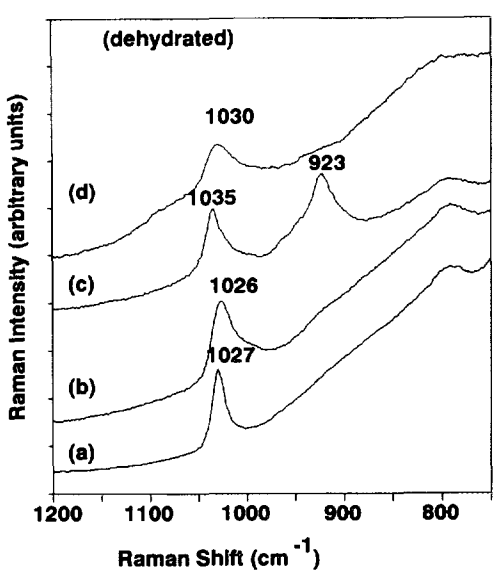

FIG. 5. Raman spectra of phosphorous-doped 1% V_2O_5/TiO_2 system. Spectra obtained under dehydrated conditions. (a) 1% V_2O_5/TiO_2; (b) 1% P_2O_5/1% V_2O_5/TiO_2; (c) 3% P_2O_5/1% V_2O_5/TiO_2; (d) 1% V_2O_5/5% P_2O_5/TiO_2.

in the 700–1200 cm^{-1} region (14). The conclusive evidence of bulk α_1-$VOPO_4$ in the 3% P_2O_5/1% V_2O_5/TiO_2 sample can only be confirmed by the application of other characterization techniques. The Raman spectrum of 1% V_2O_5 on previously prepared 5% P_2O_5/TiO_2 only possesses a broad band at 1035 cm^{-1}. The Raman spectra of the 1% P_2O_5/1% V_2O_5/TiO_2 and 1% V_2O_5/5% P_2O_5/TiO_2 samples obtained under ambient conditions reveal Raman bands at ~973 and ~984 cm^{-1}, respectively, and are different from the corresponding spectra obtained under dehydrated conditions.

Methanol Oxidation

Additives on titania. The methanol oxidation activities (A_c) and selectivities to formaldehyde (HCHO), dimethyl ether (DME), dimethoxy methane (DMM), methyl formate (MF), and carbon oxides (CO_x) of different oxides (used in this study) supported on TiO_2 support are shown in Table 2 along with data for the 1% V_2O_5/TiO_2 sample and the pure TiO_2 support. The moles of the cation of the different supported phases are also included. Comparison of the different activities and selectivities in Table 2 reveals that the surface vanadium oxide species forms the redox sites and that the redox activity (A_c × selectivity of HCHO) is more than three orders of magnitude greater than the redox activity of the next most active catalysts (1% K_2O/TiO_2). The rest of the catalysts show no detectable redox activity under the present conditions. The 7% WO_3/TiO_2 and 5% P_2O_5/TiO_2 samples show an increase in activity to acid products (dimethyl ether), suggesting that these additives form acidic sites, but the total activity is still less than the 1% V_2O_5/TiO_2 catalyst by greater than 1.5 orders of magnitude. The Nb_2O_5/TiO_2 catalyst shows a slight increase in the total activity compared to pure TiO_2 and dimethyl ether is the only product. The SiO_2/TiO_2 sample shows a slight decrease in the methanol oxidation activity to dimethyl ether, suggesting that part of the TiO_2 surface is exposed and/or the surface silica species is inactive toward methanol oxidation. Thus, the reactivity of the series of additives on 1% V_2O_5/TiO_2 catalysts is dominated by the redox properties of the surface vanadia species, and the influence of the additives upon the surface vanadium oxide species can be determined.

Niobia–vanadia–titania. The effect of adding different amounts of niobia to the 1% V_2O_5/TiO_2 sample to methanol oxidation turnover frequency (TOF) is shown in Table 3. The TOF for the 1% V_2O_5/TiO_2 sample is 2.0 s^{-1} and is included for reference. The selectivity of all these samples is greater than 96% to formaldehyde. No appreciable change in the TOF (1.5–1.6 s^{-1}) for methanol oxidation is observed for addition of up to 6% Nb_2O_5 by the aqueous impregnation method. In addition, no appreciable change in the TOF (1.4–1.8 s^{-1}) is observed when

TABLE 2

Activity and Selectivity of Additives on TiO_2, 1% V_2O_5/TiO_2, and TiO_2

Sample	A_c[a]	Mole[b] ($\times 10^4$/g)	Selectivity (%) FA	MF	DMM	DME	CO_x
3.0% Nb_2O_5/TiO_2	0.007	2.26	—	—	—	100	—
5.0% Nb_2O_5/TiO_2[c]	0.006	3.76	—	—	—	100	—
7.0% WO_3/TiO_2	0.013	3.02	—	—	—	100	Tr
3.0% SiO_2/TiO_2	0.001	5	—	—	—	100	—
1.0% K_2O/TiO_2	0.005	2.13	10	—	—	89	1
5.0% P_2O_5/TiO_2	0.015	7.04	—	—	—	100	—
1.0% V_2O_5/TiO_2	0.81	1.10	99	—	—	Tr	—
TiO_2	0.002	—	—	—	—	91	9

[a] Moles of methanol converted per gram catalyst per hour.
[b] Mole of deposited cation based on weight percent oxide.
[c] From Ref (11).

the sequence of impregnation of vanadium oxide and niobium oxide are reversed or the niobium oxide precursor (niobium ethoxide/niobium oxalate) is changed.

Tungsten oxide–vanadia–titania and silica–vanadia–titania. The effect on the TOF for methanol oxidation is shown in Table 4 as tungsten oxide and silica are added to the previously prepared 1% V_2O_5/TiO_2 sample. The TOF of 1% V_2O_5/TiO_2 is included for reference. The selectivity of all of the samples is greater than 93% to formaldehyde. From Table 3 it is observed that the TOF for methanol oxidation is unaffected by the addition of tungsten oxide or silica. Reversing the sequence of depositing tungsten oxide and vanadium oxide shows similar TOF values.

Potassium oxide–vanadia–titania. Table 5 shows the TOF for methanol oxidation of the potassium-doped 1% V_2O_5/TiO_2 samples. Upon addition of potassium to the 1% V_2O_5/TiO_2 sample a gradual decrease in the TOF for methanol oxidation is observed and an order of magnitude decrease of the oxidation activity (TOF) occurs upon addition of 0.7% K_2O to the 1% V_2O_5/TiO_2 sample. An increase in the selectivity toward carbon oxides is also observed for greater than 0.7% amounts of K_2O on the 1% V_2O_5/TiO_2 sample.

Phosphorous oxide–vanadia–titania. The effect of the addition of phosphorous to the 1% V_2O_5/TiO_2 sample on the TOF and selectivity of methanol oxidation is shown in Table 6. Addition of 1% P_2O_5 results in a slight decrease in the methanol oxidation turnover frequency and a corresponding slight increase in the selectivity to dimethyl ether. Addition of 3% P_2O_5 to a previously prepared 1% V_2O_5/TiO_2 sample shows a drastic change in the TOF and selectivity. The TOF for the 3% P_2O_5/1% V_2O_5/TiO_2 sample, 6.4×10^{-2} s^{-1}, is about two orders of magnitude less than the TOF of the 1% V_2O_5/TiO_2 sample, 2.0×10^0 s^{-1}, and the selectivity of the 3% P_2O_5/1% V_2O_5/TiO_2

TABLE 3

The TOF for Methanol Oxidation of Niobia-Doped 1% V_2O_5/TiO_2 Samples

Sample	TOF[a]	Selectivity (%) FA	DMM	DME	CO_x
1% V_2O_5/TiO_2	2.0	99	—	Tr	—
3% Nb_2O_5/1% V_2O_5/TiO_2 (aqueous prep.)	1.5	97	3	Tr	—
6% Nb_2O_5/1% V_2O_5/TiO_2 (aqueous prep.)	1.6	96	3	1	—
6% Nb_2O_5/1% V_2O_5/TiO_2 (nonaqueous prep.)	1.8	97	2	1	—
1% V_2O_5/3% Nb_2O_5/TiO_2 (nonaqueous prep.)	1.4	96	3	1	—

[a] Based on total activity.

TABLE 4

The TOF for Methanol Oxidation of Silica- and Tungsten Oxide-Doped 1% V_2O_5/TiO_2 Samples

Sample	TOF[a]	Selectivity (%) FA	DMM	DME	CO_x
1% V_2O_5/TiO_2	2.0	99	—	Tr	—
3% SiO_2/1% V_2O_5/TiO_2	2.7	96	3	Tr	Tr
7% WO_3/1% V_2O_5/TiO_2	3.4	93	5	2	—
1% V_2O_5/7% WO_3/TiO_2	2.0	99	1	Tr	—

[a] Based on total activity.

TABLE 5

The TOF for Methanol Oxidation of Potassium Oxide-Doped 1% V_2O_5/TiO_2 Samples

Sample	A_c[a]	TOF[b] (s^{-1})	Selectivity (%)				
			FA	MF	DMM	DME	CO_x
0.04% K_2O/1% V_2O_5/TiO_2	0.960	2.4	97	—	2	Tr	Tr
0.16% K_2O/1% V_2O_5/TiO_2	0.460	1.2	99	—	—	Tr	—
0.3% K_2O/1% V_2O_5/TiO_2	0.200	0.5	100	—	—	—	—
0.7% K_2O/1% V_2O_5/TiO_2	0.026	0.07	100	—	—	Tr	—

[a] Moles of methanol converted per gram catalyst per hour.
[b] Based on total activity (A_c).

sample is 52% to dimethyl ether compared to negligible amounts of dimethyl ether (<1%) for the undoped sample. The addition of 1% V_2O_5 to a previously prepared 5% P_2O_5/TiO_2 sample shows a different behavior toward methanol oxidation. The methanol oxidation TOF for 1% V_2O_5/5% P_2O_5/TiO_2 ($\sim 1.0 \times 10^{-1}\ s^{-1}$) is an order of magnitude less than that for the 1% V_2O_5/TiO_2 sample. In addition, the selectivity of methanol toward dimethyl ether of the 1% V_2O_5/5% P_2O_5/TiO_2 sample is ~15%.

DISCUSSION

In order to understand the effect of additives on the 1% V_2O_5/TiO_2 sample, it is worthwhile first to discuss the structure and reactivity relationship of the unpromoted V_2O_5/TiO_2 system as a function of vanadium oxide loading.

Under ambient conditions, where moisture is present, metavanadate and decavanadate species are observed on the TiO_2 support (15, 16). The relative ratio of the two vanadium oxide species on TiO_2 depends on the surface vanadium oxide loading—the decavanadate species is predominantly present at monolayer coverages (>95%). The maximum vanadium oxide loading that can be deposited on the TiO_2 support (Degussa P-25, 55 m^2/g) as a molecular dispersed phase corresponds to 6% V_2O_5 (8, 12).

Upon dehydration, a change in the Raman spectra (8, 12) and solid state ^{51}V NMR spectra (16) is observed, and four coordinated species on the surface of TiO_2 were proposed for low vanadium oxide loadings (1% V_2O_5/TiO_2). For low vanadium oxide loadings, the Raman spectra are dominated by a band at 1027 cm^{-1}, and at high loadings, an additional band at 920–930 cm^{-1} is observed (8, 12, 17, 18). The 920–930 cm^{-1} band has been assigned to a polymerized surface vanadium oxide species by many investigators (8, 17–19). The ratio of these two Raman bands of the dehydrated catalysts is a function of vanadium oxide loading. The dehydrated structure of the surface vanadium oxide species is used for the structure–reactivity relationship since under reaction conditions (200–400°C) the surface moisture present under ambient conditions desorbs. The methanol oxidation turnover frequency (TOF) shows a similar value of 1.1–2.7 s^{-1} for the 1–6% V_2O_5/TiO_2 samples with a selectivity of more than 95% to formaldehyde (20) suggesting the insensitivity of methanol oxidation to the ratio of the 1027–1030 and 920–930 cm^{-1} bands. Bulk V_2O_5, in comparison, possesses a TOF of $2.2 \times 10^{-2}\ s^{-1}$ for methanol oxidation (21).

Under ambient conditions, the surface of the oxide sup-

TABLE 6

The TOF for Methanol Oxidation of Phosphorous Oxide-Doped 1% V_2O_5/TiO_2 Samples

Sample	A_c[a]	TOF[b] (s^{-1})	Selectivity (%)				
			FA	MF	DMM	DME	CO_x
1% P_2O_5/1% V_2O_5/TiO_2	0.520	1.3	92	—	6	Tr	—
3% P_2O_5/1% V_2O_5/TiO_2	0.025	0.06	25	—	—	52	23
1% V_2O_5/5% P_2O_5/TiO_2	0.066	0.17	74	—	13	13	—

[a] Moles of methanol converted per gram catalyst per hour.
[b] Based on total activity (A_c).

port possess a film of water, and the structure of the surface vanadium oxide phase is controlled by the pH at pzc of the water film (15). Addition of additives to the 1% V_2O_5/TiO_2 sample changes the pH at pzc of the surface water film and, consequently, changes the structure of the surface vanadium oxide phase as would be expected from the aqueous phase diagram (22). A lower pH, or acidic additive, would dictate more polymerized and six coordinated vanadium oxide structures (the decavanadate ion and its corresponding hydrated analogues) to be present. A higher pH, or basic additive, would dictate isolated and four coordinated surface vanadium oxide species (orthovanadate ion and its corresponding hydrated analogues) to be present. Indeed, upon addition of tungsten oxide, phosphorous oxide, and niobia, the structure of the surface vanadium oxide species becomes predominantly six coordinated as reflected by the upward shift of the Raman band from ~950 to 970–980 cm^{-1} upon addition of these additives to the 1% V_2O_5/TiO_2 sample. Addition of potassium to the 1% V_2O_5/TiO_2 sample, however, results in a gradual decrease in the Raman band from ~940 to 880 cm^{-1}. No change of the Raman spectra of the surface vanadium oxide species is observed for the silica-doped 1% V_2O_5/TiO_2 sample, contrary to what is expected for acidic additives. Thus, under ambient conditions the additives can be classified as acidic (WO_3, Nb_2O_5, and P_2O_5) and basic (K_2O), and the structure of the surface vanadium oxide species is controlled by the net surface pH at pzc. The behavior of silica as an additive to the 1% V_2O_5/TiO_2 system does not follow any trend and may be classified as neutral. The 3% P_2O_5/1% V_2O_5/TiO_2 sample is an exception to the net surface pH at pzc behavior since a vanadium phosphate microcrystalline compound is formed, which is not a two-dimensional phase.

In situ dehydration results in the removal of surface moisture, and the structure of the vanadium oxide species is no longer controlled by the pH at pzc of the surface moisture layer. Therefore, the structure of the surface vanadium oxide species no longer controls the reactivity and the dehydrated surface vanadium oxide structure is more closely related to the reactivity information. The Raman spectra (Figs. 1–5) and methanol oxidation results (Tables 3–6) of the various additives on the 1% V_2O_5/TiO_2 sample indicate two types of interactions that exist. Addition of tungsten oxide, niobia, and silica does not significantly affect the terminal oxygen (V=O) vibration of the dehydrated surface vanadium oxide phase. Addition of tungsten oxide and niobia gives rise to an additional Raman band at 920–930 cm^{-1}, which is similar to the effect of increasing the vanadium oxide loading of the V_2O_5/TiO_2 system. However, by comparison the increase in the 920–930-cm^{-1} Raman band is much smaller than the same band present at monolayer V_2O_5 loadings on TiO_2 (6% V_2O_5/TiO_2). The behavior of silica toward the surface vanadium oxide phase is slightly different from that toward tungsten oxide and niobia since no 920–930 cm^{-1} band is observed and the V=O terminal bond decreases from 1027 to 1024 cm^{-1}. Consequently, these additives (WO_3, Nb_2O_5, and SiO_2) seem to interact directly with the support, and in some cases (WO_3 and Nb_2O_5) result in the same effect as artificially increasing the vanadium oxide loading and the formation of the second vanadium oxide species that possesses the 920–930 cm^{-1} Raman band. The noninteracting behavior of these additives (WO_3, Nb_2O_5, and SiO_2) with the surface vanadium oxide phase is substantiated by the methanol oxidation studies since no detectable change in the TOF is observed and the selectivity remains primarily to formaldehyde. The additives on TiO_2, in the absence of the surface vanadium oxide phase, are essentially inactive in the partial oxidation of methanol (Table 2). Based on the structure–reactivity information a model can be developed summarizing these observations, illustrated in Fig. 6.

The model in Fig. 6 shows that the isolated four coordinated vanadium oxide species, the predominant species in the 1% V_2O_5/TiO_2 sample (Raman band 1027–1030 cm^{-1}), remains essentially unaffected upon addition of the noninteracting additives (M_xO_y). Formation of the second species (Raman band at 920–930 cm^{-1}) is also observed in the Raman spectra of some of the noninteracting additives (WO_3 and Nb_2O_5) on the 1% V_2O_5/TiO_2 sample, but the second species only form a minor fraction. The formation of the second species, however, would not be expected to change the TOF for methanol oxidation since the TOF is not a function of vanadium oxide coverage. In addition, the preparation method and sequence of preparation of the noninteracting additives do not change the structure or reactivity of the surface vanadium oxide phase. No compound formation of these additives (WO_3, Nb_2O_5, and SiO_2) with the surface vanadium oxide phase is observed, nor is any crystal formation of these additives or the surface vanadium oxide phase detected.

The addition of potassium has a more pronounced effect on the surface vanadium oxide species as is evident from the Raman spectra of the potassium-doped 1% V_2O_5/TiO_2 samples (Fig. 4). Addition of potassium to the 1% V_2O_5/

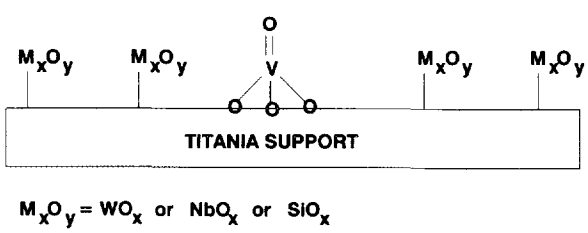

FIG. 6. Model of noninteracting additives with the surface vanadium oxide species on titania. Noninteracting additives denoted as M_xO_y, where M_xO_y = WO_x, NbO_x, or SiO_x.

TiO_2 sample results in a decrease in the Raman band of the V=O bond to a lower wavenumber, which corresponds to an increase in the bond length of the terminal V=O bond (23). New Raman bands simultaneously develop in the 900–1000 cm^{-1} region, suggesting the formation of additional species. Solid-state ^{51}V NMR dehydration studies indicate that the surface vanadium oxide species is four coordinated for the potassium-doped 1% V_2O_5/TiO_2 samples with a growth of a shoulder at ~−550 ppm (polymeric four coordinated vanadium oxide structure) in addition to the ~−660-ppm peak of the undoped dehydrated surface vanadium oxide sample (24). It should be noted that none of the Raman bands observed under dehydrated conditions is similar to the Raman bands observed under hydrated conditions, which suggests that no microcrystalline compounds are formed at these levels of potassium and vanadium oxide. This is the first direct structural evidence that the potassium oxide coordinates with the surface vanadium oxide phase but does not form microcrystalline compounds.

The interaction of potassium with the surface vanadium oxide phase is also reflected by the methanol oxidation experiments. Addition of potassium results in the decrease in the TOF caused by poisoning of the surface vanadium oxide redox sites. The exact interaction method of potassium with the surface vanadium oxide site is currently not clear. Potassium definitely decreases the bond strength of the V=O bond since the Raman spectra of the potassium-doped 1% V_2O_5/TiO_2 samples possess Raman bands lower than 1027 cm^{-1}. It also must affect the vanadium–oxygen–support bridging bond since this bond controls the reactivity of the V_2O_5/TiO_2 samples for methanol oxidation (21). The most probable model of this interacting additive (potassium) with the surface vanadium oxide species on titania is shown in Fig. 7, where the potassium ion is shown to interact with the terminal V=O bond and/or the vanadium–oxygen–support bridging bond.

The addition of phosphorous to the 1% V_2O_5/TiO_2 catalyst is the most complicated of the additives studied since the order of addition of the supported oxide phases is critical. Small amounts of phosphorous (1% P_2O_5) do not appear to affect most of the surface vanadium oxide species since the vanadium oxide vibration still exists at

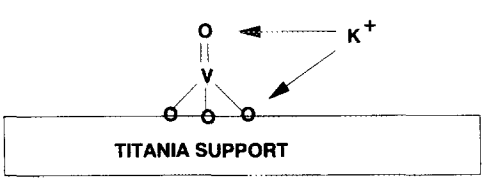

FIG. 7. Model of interacting additives (potassium) with the surface vanadium oxide species on titania.

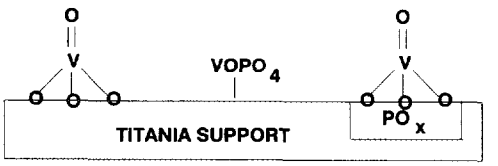

FIG. 8. Model of interacting additives (phosphorous) with the surface vanadium oxide species on titania.

~1027 cm^{-1}. This is substantiated by the solid-state ^{51}V NMR (24) and the methanol oxidation studies since no additional vanadium oxide structures are observed, and only a slight decrease in the TOF is detected. Additional amounts of phosphorous, however, result in the formation of microcrystalline vanadium phosphate compounds since the Raman spectra upon hydration and dehydration experiments are the same. The methanol oxidation reaction reveals a decrease in TOF and an increase in dimethyl ether selectivity, which also suggests the formation of a different catalytic active site.

Changing the sequence of preparation, e.g., by depositing 1% V_2O_5 on a previously prepared 5% P_2O_5/TiO_2 sample, results in a different Raman spectrum and methanol oxidation activity. No compound formation is observed for the 1% V_2O_5/5% P_2O_5/TiO_2 sample since the Raman spectra change during hydration and dehydration experiments. In perspective, the Raman spectra of the P_2O_5/TiO_2 system do not change during hydration and dehydration experiments, and suggest a strong interaction (compound formation) of phosphorous oxide with the TiO_2 support (25). The methanol oxidation data show that the deposition of 1% V_2O_5 on the 5% P_2O_5/TiO_2 sample results in a decrease in the TOF. The TOF for methanol oxidation of the V_2O_5/TiO_2 system is controlled by the vanadium–oxygen–titanium bond (21), and the decrease in TOF and the strong interaction of phosphorous oxide with the TiO_2 support in the P_2O_5/TiO_2 system suggest that part or all of the phosphorous oxide phase is present near the surface. Thus, the surface vanadium oxide phase appears to form vanadium–oxygen–phosphorous bonds with the surface phosphorous oxide phase, which would explain the decrease in the methanol oxidation TOF. The difference in the Raman spectra and methanol oxidation activity/selectivity data on changing the sequence of impregnation of phosphorous and vanadia on titania suggests that the phosphorous oxide does not discriminate between the TiO_2 surface or the surface vanadium oxide phase and interacts strongly with both. The model of the phosphorous interaction with 1% V_2O_5/TiO_2 sample is illustrated in Fig. 8. Figure 8 tentatively explains the behavior of phosphorous with the surface vanadium oxide phase as described above.

This study establishes the effect of additives on the

structure and reactivity of the surface vanadium oxide phase on titania. Recent studies have shown that similar behavior is observed for additives on different oxide supports (Al_2O_3) and higher vanadium oxide loadings. Thus, the interacting and noninteracting behavior of the additives is not restricted to the 1% V_2O_5/TiO_2 system (26, 27). While studying the oxidation activity of promoted supported vanadium oxide catalysts, however, other factors usually need to be considered when relating the above information. For example, the surface acidity may provide certain critical reactivity parameters in addition to the redox activity of the surface vanadium oxide phase for determining the overall reactivity of additives on supported vanadium oxide catalysts (4, 10). Such factors are not considered in this study. However, the behavior of interacting and noninteracting additives toward the surface redox vanadium oxide site in the V_2O_5/TiO_2 system is a major step in forming a basis for understanding the effect of additives on supported vanadium oxide catalysts.

CONCLUSIONS

The effect of additives on the structure and reactivity of the surface vanadium oxide phase on low loading V_2O_5/TiO_2 samples was successfully studied by Raman spectroscopy and the methanol oxidation, respectively. Under ambient conditions, the effect of the additives is to change the pH at pzc of the surface moisture layer and change the structure of the surface vanadium oxide depending on the aqueous acid/base characteristic of the additives. The Raman spectra of the dehydrated samples and methanol oxidation behavior of the various additives on the 1% V_2O_5/TiO_2 sample reveal that there are essentially two types of interactions between the additives and the surface vanadium oxide phase. Noninteracting additives (WO_3, Nb_2O_5, and SiO_2) do not significantly affect the structure of the surface vanadium oxide phase, and no change in the methanol oxidation activity or selectivity of the surface vanadium oxide phase is observed. The order of impregnation or preparation method of the noninteracting additive does not affect the structure or methanol oxidation activity of the surface vanadium oxide phase. Interacting additives (P_2O_5 and K_2O), however, have a pronounced effect on the structure and reactivity of the surface vanadium oxide phase. The addition of potassium to the V_2O_5/TiO_2 sample gradually poisons the surface vanadium oxide redox site. This is reflected in changes in the Raman spectra and a decrease in methanol oxidation activity. The effect of phosphorous on the V_2O_5/TiO_2 sample depends on the sequence of impregnation. When phosphorous is deposited on a previously prepared V_2O_5/TiO_2 sample, the Raman spectra suggest that a vanadium phosphate compound is formed at high phosphorous loadings, and a decrease in methanol oxidation activity as well as an increase in selectivity to dimethyl ether is observed. When vanadium oxide is deposited on a previously prepared P_2O_5/TiO_2 sample, no compound formation is indicated from Raman spectroscopy, but a corresponding decrease in the methanol oxidation activity suggests that the poisoning of the surface vanadium oxide site occurs, presumably by the formation of vanadium–oxygen–phosphorous bonds.

ACKNOWLEDGMENT

The Financial support of NSF Grant CTS-9006258 is gratefully acknowledged.

REFERENCES

1. Wainwright, M. S., and Foster, N. R., *Catal. Rev.* **19,** 211 (1979).
2. Bond, G. C., and Brukman, B. K., *Faraday Discuss. Chem. Soc.* **72,** 235 (1981).
3. Eckert, H., Deo, G., Wachs, I. E., and Hirt, A. M., *Colloids Surf.* **45,** 347 (1990).
4. van Hengstum, A. J., Pranger, J., van Ommen, J. G., and Gellings, P. J., *Appl. Catal.* **11,** 317 (1984).
5. Zhu, J., and Andersson, S. L. T., *J. Chem. Soc., Faraday Trans. 1* **85**(1), 3629 (1989).
6. Zhu, J., and Andersson, S. L. T., *J. Chem. Soc., Faraday Trans. 1* **85**(1), 3645 (1989).
7. Bond, G. C., and Tahir, S. F., *Catal. Today* **10,** 393 (1991).
8. Vuurman, M. A., Hirt, A. M., and Wachs, I. E., *J. Phys. Chem.* **95,** 9928 (1991).
9. Ramis, G., Busca, G., and Forzatti, P., *Appl. Catal. B: Environmental* **1,** L9 (1992).
10. Chen, J. P., and Yang, R. T., *Appl. Catal. A: General* **80,** 135 (1992).
11. Jehng, J.-M., and Wachs, I. E. *J. Phys. Chem.* **95,** 7373 (1991).
12. Deo, G., and Wachs, I. E., submitted for publication.
13. Jehng, J.-M., Deo, G., and Wachs, I. E., unpublished results.
14. Ben Abdelouahab, F., Olier, R., Guilhaume, N., Lefebvre, F., and Volta, J. C., *J. Catal.* **134,** 151 (1992).
15. Deo, G., and Wachs, I. E., *J. Phys. Chem.* **95,** 5889 (1991).
16. Eckert, H., and Wachs, I. E., *J. Phys. Chem.* **93,** 6796 (1989).
17. Went, G. T., Leu, L.-J., Rosin, R., and Bell, A. T., *J. Catal.* **134,** 479 (1992).
18. Cristiani, C., Forzatti, P., and Busca, G., *J. Catal.* **116,** 586 (1989).
19. Wachs, I. E., *J. Catal.* **124,** 570 (1991).
20. Deo, G., and Wachs, I. E., *J. Catal.* **146,** 323 (1994).
21. Deo, G., and Wachs, I. E., *J. Catal.* **129,** 307 (1991).
22. Baes, C. F., Jr., and Mesmer, R. E. *in* "The Hydrolysis of Cations," Krieger, Florida, 1986.
23. Hardcastle, F. D., and Wachs, I. E., *J. Phys. Chem.* **95,** 5031 (1991).
24. Eckert, H., Deo, G., and Wachs, I. E., unpublished results.
25. Hardcastle, F. D., Turek, A. M., and Wachs, I. E., unpublished results.
26. Deo, G., and Wachs, I. E., unpublished results.
27. Vuurman, M., and Wachs, I. E. *J. Mol. Catal.* **77,** 29 (1992).